

Mechanism of Hydrolysis of Isopropenyl Glucopyranosides. Spectroscopic Evidence Concerning the Greater Reactivity of the α Anomer[†]

H. Keith Chenault* and Laura F. Chafin

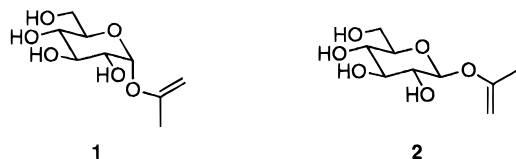
Department of Chemistry and Biochemistry, University of Delaware, Newark, Delaware 19716

Received November 19, 1997

The mechanism of hydrolysis of isopropenyl α - and β -glucopyranosides (**1** and **2**, respectively) has been studied by temperature-dependent reaction kinetics, stereochemical analysis of products by ¹H NMR, solvent ¹⁸O- and ²H-labeling experiments, kinetic solvent deuterium isotope effects, and α -values for general acid catalysis. Compounds **1** and **2** are the first vinyl acetals to be shown to undergo hydrolysis exclusively by cleavage of the vinyl ether and not the acetal C–O bond. While both glucopyranosides undergo irreversible, rate-limiting C-protonation, **1** hydrolyzes approximately four times faster than **2** and has an enthalpy of activation that is 5.8 kcal mol⁻¹ lower than that of **2**, suggesting that **1** is kinetically more basic than **2**. Spectroscopic evidence indicates that conjugation of the glycosidic oxygen with the alkenyl double bond is greater in **1** than in **2**, probably because of steric or conformational constraints.

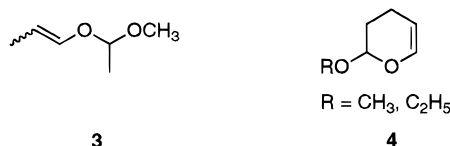
Introduction

As part of an investigation of isopropenyl glycosides as potential substrates for enzyme-catalyzed¹ and electrophile-mediated² transglycosylation reactions, we have examined the mechanism and rates of hydrolysis of isopropenyl α -D-glucopyranoside (**1**) and its β anomer (**2**).³



Before our work, it was not apparent whether hydrolysis of these vinyl glycosides would proceed with cleavage of the glycosidic (acetal) or vinyl ether C–O bond. Propenyl acetals, such as **3**, hydrolyze with exclusive cleavage of the acetal C–O bond.⁴ On the other hand, hydrolysis of 2-alkoxy-2,3-dihydropyrans, such as **4**, involves competing cleavage of both acetal and vinyl ether moieties.^{5,6} The rate of acetal hydrolysis in **4** may be attenuated by intramolecular collapse of the oxocarbenium ion with the enol leaving group.

Another point to be studied was whether the anomeric configuration of **1** or **2** influences the rate or mechanism of hydrolysis. The α and β anomers of alkyl glycopyranosides and related compounds are known to differ in the rates at which they undergo hydrolysis,⁷ oxidation,^{8,9}



hydrogen atom abstraction,¹⁰ and substitution by Grignard reagents.¹¹ In the case of hydrolysis, the differences in rates of reaction are often relatively small. Alkyl β -glycosides hydrolyze 1.3–3.2 times faster than their corresponding α anomers, and aryl α -glycopyranosides hydrolyze 4.1–8.7 times faster than their corresponding β -glycopyranosides.¹² Considerable controversy surrounds the mechanistic explanations for these small rate differences.^{13–17} It is unclear whether the primary influence of $n_O \rightarrow \sigma^*_{CO}$ orbital interactions is on ground states or transition states of the reactions. Additionally, the influence of the anomeric effect on the equilibrium populations of various protonated and twist-boat intermediates adds another layer of uncertainty to the problem.^{9,18}

[†] This paper is dedicated to Professor Melvyn D. Schiavelli on the occasion of his 55th birthday.

(1) Castro, A. Ph.D. Dissertation, University of Delaware, 1995, Chapter 1.

(2) (a) Chenault, H. K.; Castro, A. *Tetrahedron Lett.* **1994**, *35*, 9145–9148. (b) Chenault, H. K.; Castro, A.; Chafin, L. F.; Yang, J. *J. Org. Chem.* **1996**, *61*, 5024–5031.

(3) Chenault, H. K.; Chafin, L. F. *J. Org. Chem.* **1994**, *59*, 6167–6169.

(4) Chiang, Y.; Chwang, W. K.; Kresge, A. J.; Yin, Y. *J. Am. Chem. Soc.* **1989**, *111*, 7185–7190.

(5) Kankaanperä, A. *Acta Chem. Scand.* **1969**, *23*, 1465–1470.

(6) Burt, R. A.; Chiang, Y.; Kresge, A. J. *Can. J. Chem.* **1980**, *58*, 2199–2202.

(7) Feather, M. S.; Harris, J. F. *J. Org. Chem.* **1965**, *30*, 153–157.

(8) (a) Isbell, H. S. *J. Res. Nat. Bureau Standards* **1962**, *66*, 233–239. (b) Angyal, S. J.; James, K. *Aust. J. Chem.* **1970**, *23*, 1209–1221.

(c) Deslongchamps, P.; Moreau, C. *Can. J. Chem.* **1971**, *49*, 2465–2467.

(d) Deslongchamps, P.; Moreau, C.; Fréhel, D.; Atlani, P. *Can. J. Chem.* **1972**, *50*, 3402–3404.

(9) Deslongchamps, P. *Pure Appl. Chem.* **1993**, *65*, 1161–1178.

(10) Remy, G.; Cottier, L.; Descotes, G. *Can. J. Chem.* **1980**, *58*, 2660–2665.

(11) Eliel, E. L.; Nader, F. W. *J. Am. Chem. Soc.* **1970**, *92*, 584–590.

(12) Capon, B. *Chem. Rev. (Washington, D.C.)* **1969**, *69*, 407–498.

(13) *The Anomeric Effect and Associated Stereoelectronic Effects*; Thatcher, G. R. J., Ed.; ACS Symposium Series 539; American Chemical Society: Washington, DC, 1993.

(14) Deslongchamps, P. *Stereoelectronic Effects in Organic Chemistry*; Pergamon: New York, 1983.

(15) Kirby, A. J. *The Anomeric Effect and Related Stereoelectronic Effects at Oxygen*; Springer-Verlag: New York, 1983.

(16) (a) Sinnott, M. L. *Adv. Phys. Org. Chem.* **1988**, *24*, 113–204.

(b) Sinnott, M. L. *Chem. Rev. (Washington, D.C.)* **1990**, *90*, 1171–1202.

(17) Ratcliffe, A. J.; Mootoo, D. R.; Andrews, C. W.; Fraser-Reid, B.

J. Am. Chem. Soc. **1989**, *111*, 7661–7662.

(18) Deslongchamps, P. In ref 13, pp 26–54.

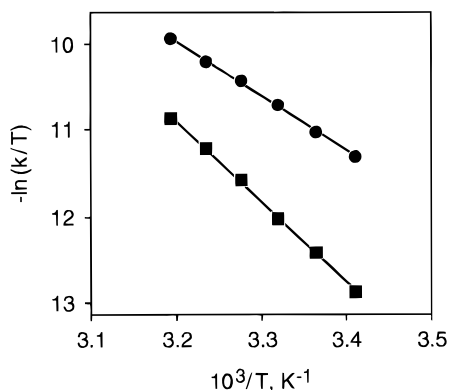


Figure 1. Eyring plots for the hydrolysis of **1** (●) and **2** (■) in 1.00 mM HCl, $I = 0.100$ M, at 20–40 °C. Data points are the averages of three determinations.

We report here that, at pH 3.0 and 25 °C, both **1** and **2** hydrolyze exclusively by irreversible, rate-limiting protonation of the β -carbon of the enol ether followed by alkenyl ether C–O bond cleavage, not glycosidic C–O bond cleavage. Compounds **1** and **2** are the first alkyl vinyl acetals reported to hydrolyze exclusively by cleavage of the vinyl ether C–O bond. Furthermore, compounds **1** and **2** exhibit a kinetic anomeric effect, with **1** hydrolyzing approximately four times faster than **2**. UV, ^1H and ^{13}C NMR, and IR spectroscopies indicate that, in the ground state, conjugation of the vinyl ether of **1** is greater than that of **2**, probably as a result of steric or conformational constraints.

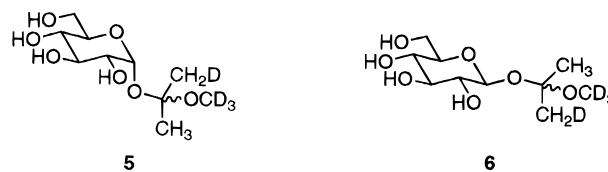
Results and Discussion

Kinetics. Isopropenyl glucopyranosides **1** and **2** were prepared as previously reported.³ Hydrolyses were performed in dilute (0.5–4.0 mM) hydrochloric or perchloric acid or in dilute (1–25 mM) solutions of carboxylic acid buffers, pH 3–4. The ionic strength (I) of solutions was typically maintained at 0.100 M by addition of NaCl. Although initial reactions were monitored by enzymatic assay for the release of glucose,³ the rates of later reactions were measured more conveniently by observing the decrease in absorbance at 215 nm due to the cleavage of the vinyl ether. Rates of hydrolysis were first order with respect to the glucopyranoside for at least 4 half-lives and were found to be first-order with respect to hydronium ion by varying the concentration of acid. At 25 °C, $[\text{H}^+] = 1.00$ mM and $I = 0.002$ M, rate constants for the hydrolysis of **1** and **2** were $(5.11 \pm 0.07) \times 10^{-3}$ and $(1.50 \pm 0.06) \times 10^{-3} \text{ s}^{-1}$, respectively. At $I = 0.100$ M, the corresponding rate constants for **1** and **2** were $(3.64 \pm 0.04) \times 10^{-3}$ and $(0.960 \pm 0.009) \times 10^{-3} \text{ s}^{-1}$, respectively. These rate constants are 10–100 times greater than those for the hydrolysis of alkyl and aryl glucosides at 60 °C and pH 0.0.¹²

Depending on the reaction conditions, **1** hydrolyzes approximately four times faster than **2**. Although this difference in reactivity corresponds to a relatively small change in free energy of activation, temperature-dependent kinetics reveal a notable difference between the enthalpies of activation for the hydrolyses of **1** and **2** (Figure 1). At 25 °C, $[\text{H}^+] = 1.00$ mM and $I = 0.100$ M, the activation parameters for the hydrolysis of **1** are $\Delta H^\ddagger = 12.56 \pm 0.21 \text{ kcal mol}^{-1}$ and $\Delta S^\ddagger = -26.8 \pm 0.7 \text{ eu}$. The corresponding activation parameters for **2** are

$\Delta H^\ddagger = 18.39 \pm 0.27 \text{ kcal mol}^{-1}$ and $\Delta S^\ddagger = -10.0 \pm 0.9 \text{ eu}$. Thus, the greater reactivity of **1** is due to a significantly lower enthalpy of activation that is only partially offset by a more negative entropy of activation.

Vinyl Ether C–O Bond Cleavage. Chemoselective hydrolysis of the vinyl ether of **1** and **2** was first suggested by the observation made by ^1H NMR that **1** hydrolyzes exclusively to give α -glucopyranose as the initially formed product while **2** hydrolyzes exclusively to give β -glucopyranose as the initially formed product.³ This result would be hard to explain if hydrolysis were proceeding by cleavage of the glycosidic (acetal) C–O bond. Reaction of **1** and **2** in methanol- d_4 containing 1 mM DCl resulted in the addition of methanol- d_4 across the alkenyl ether double bond to form glucosyl methyl acetones **5** and **6**, respectively, as products and not methyl glucopyranosides. Again, this result is consistent with a mechanism of hydrolysis involving cleavage of the vinyl ether C–O bond and not cleavage of the glycosidic C–O bond.



To prove unequivocally which C–O bond is cleaved during hydrolysis, **1** and **2** were hydrolyzed in $[\text{18O}]$ water (97.9%), and aliquots were analyzed by mass spectroscopy. GC-MS showed complete incorporation of one atom of solvent-derived ^{18}O into the acetone formed while electrospray-MS indicated no incorporation of ^{18}O into the glucose formed. On the basis of the relative magnitudes of the M^+ peak for acetone and the $M + 2$ peak for glucose, less than 0.5% of the hydrolysis observed involves cleavage of the acetal moiety.

Irreversibility of C-Protonation. When the electrophilic addition of methanol- d_4 to **1** and **2** was observed by ^1H NMR as described above, no deuterium was incorporated into the starting material and only one atom of deuterium was observed to be incorporated into **5** and **6**.³ Similarly, when **1** and **2** were hydrolyzed in D_2O , analysis by ^1H NMR and GC-MS indicated no exchange of deuterium for vinyl protons in the starting material and incorporation of only one atom of deuterium into the acetone produced. These results indicate that protonation of the β -carbon of the enol ether of **1** and **2** is irreversible. On the basis of the magnitude of the $M + 2$ peak for the acetone produced, less than 0.5% of the hydrolysis proceeds with incorporation of two atoms of deuterium into product.

Kinetic Solvent Deuterium Isotope Effects. When the hydrolyses of **1** and **2** in buffered D_2O were observed by ^1H NMR, the rates appeared to be more than six times slower than those measured under essentially identical conditions in H_2O . Careful spectrophotometric measurement of the rates of hydrolysis of **1** and **2** at 25 °C in H_2O and D_2O solutions of 10 mM chloroacetate buffer, at a nominal pH of 3.0, confirmed this finding. Apparent solvent deuterium isotope effects for **1** and **2** were 7.66 ± 0.25 and 7.56 ± 0.47 , respectively. Taking into account

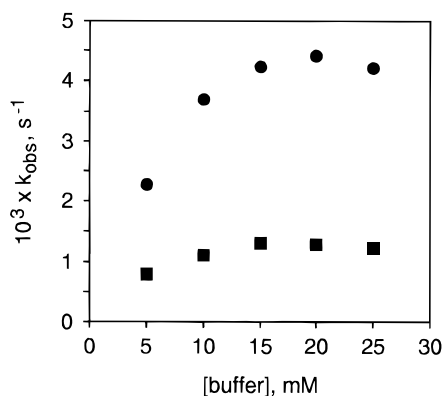


Figure 2. Observed rate constants for the hydrolysis of **1** (●) and **2** (■) in chloroacetate buffer, nominal pH 3.0, at 25 °C.

Table 1. Solvent Isotope Effects on the Hydrolysis of 1 and 2 at 25 °C and $I = 0.002$ M

	1	2
k_{H^+} , $M^{-1} s^{-1}$	5.11 ± 0.07	1.50 ± 0.06
k_{D^+} , $M^{-1} s^{-1}$	1.70 ± 0.03	0.480 ± 0.008
k_{H^+}/k_{D^+}	3.01 ± 0.07	3.13 ± 0.14

the differences in lyonium ion concentration¹⁹ due to the suppression of ionization of chloroacetic acid in D_2O ²⁰ and the fact that lyonium ion was the dominant catalytic species present (see below), the solvent isotope effects on catalysis by lyonium ion, k_{H^+}/k_{D^+} , were calculated to be 3.06 ± 0.10 and 3.02 ± 0.19 for **1** and **2**, respectively.

Measurement of the rates of hydrolysis of **1** and **2** in dilute solutions of perchloric acid in H_2O and D_2O allowed the catalytic rate constants, k_{H^+} and k_{D^+} , to be determined individually (Table 1). From these rate constants, the values of k_{H^+}/k_{D^+} for the hydrolysis of **1** and **2** were calculated to be 3.01 ± 0.07 and 3.13 ± 0.14 , respectively. These normal solvent deuterium isotope effects indicate rate-limiting C-protonation, and their magnitude is typical for the hydrolysis of vinyl ethers.^{5,21,22} By contrast, an inverse solvent isotope effect ($k_{H^+}/k_{D^+} < 1$) would have been expected for a process involving preequilibrium proton transfer, as is typical for acetal hydrolysis.

α Coefficients for General Acid Catalysis. Brønsted α coefficients for the hydrolyses of **1** and **2** were investigated by examining the effects of varying concentrations of carboxylic acid buffers (chloroacetic, 3-chlorolactic, formic, glycolic, and propionic) on the hydrolyses of **1** and **2**. At moderate concentrations of buffer, however, standard buffer dilution plots exhibited negative curvature that exceeded that due to normal buffer failure (Figure 2). This type of curvature has been observed by others and has been attributed to self-association of buffer components in solution.²³ At lower concentrations of buffer, the observed curvature was less

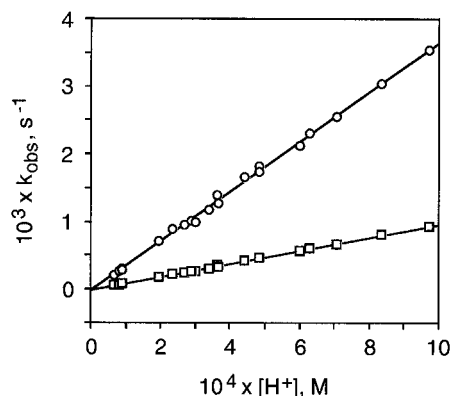


Figure 3. Observed rate constants for the hydrolysis of **1** (○) and **2** (□) in carboxylic acid buffers (1–10 mM, $I = 0.100$ M, 25 °C) plotted as a function of the actual concentration of hydronium ion.

pronounced, but the overall contribution of buffer to catalysis was so small that the rates of hydrolysis were determined largely by catalysis by the hydronium ion. Rates of hydrolysis of **1** and **2** at low concentrations (1–10 mM) of buffer exhibited essentially no dependence on the concentration of buffer. In fact, when buffer failure was taken into account, a plot of the observed rate constants versus actual concentration of hydronium ion gave a straight line, regardless of the concentrations or identities of the buffers used (Figure 3). From this plot, the values of k_{H^+} for **1** and **2** at $I = 0.100$ M were determined to be 3.67 ± 0.04 and 0.967 ± 0.008 $M^{-1} s^{-1}$, respectively. These rate constants are identical, within experimental error, with those determined by varying the concentration of mineral acid (see Kinetics above).

Another method of determining the α coefficient for general acid catalysis involves measuring the effective solvent isotope effects for a reaction run in mixtures of H_2O and D_2O .^{21,24,25} This solvent isotope effect method has been found to give values of α that are essentially identical with those determined by normal buffer dilution techniques.^{21,23,25} The agreement between the two methods is not surprising since both methods provide information about the extent to which a proton in flight has been transferred in the transition state. For a proton being transferred from the lyonium ion to a substrate containing no other exchangeable hydrogen atoms—or in which the fractionation factors for all other exchangeable hydrogens remain constant during the activation of the substrate²⁶— α can be determined from eq 1, in which χ represents the mole fraction of exchangeable deuterium contained in the solvent, k_{χ}/k_H represents the kinetic isotope effect in a solvent of deuterium content χ , and λ represents the fractionation factor for the lyonium ion, which, in this case, is 0.69.²⁷ The dependence of k_{χ}/k_H on χ is particularly sensitive to the magnitude of α for reactions in which $k_{H^+}/k_{D^+} > 2$. Hydrolysis of **1** and **2** in

(19) The concentration of lyonium ion was set by the nominal buffer ratio, $([ClCH_2CO_2H]/[ClCH_2CO_2^-])_{nom} = 0.741$, and the effective dissociation of chloroacetic acid in H_2O and D_2O .

(20) The pK_a of chloroacetic acid in D_2O is greater than that in H_2O by 0.49: (a) McDougall, A. O.; Long, F. A. *J. Phys. Chem.* **1962**, *66*, 429–433. (b) Bell, R. P.; Kuhn, A. T. *Trans. Faraday Soc.* **1963**, *59*, 1789–1793.

(21) Salomaa, P.; Kankaanperä, A.; Lajunen, M. *Acta Chem. Scand.* **1966**, *20*, 1790–1801.

(22) (a) Kresge, A. J.; Chwang, W. K. *J. Am. Chem. Soc.* **1978**, *100*, 1249–1253. (b) Kresge, A. J.; Leibovitch, M. *Can. J. Chem.* **1990**, *68*, 2129–2130. (c) Kresge, A. J.; Leibovitch, M. *J. Am. Chem. Soc.* **1992**, *114*, 3099–3102. (d) Jones, J.; Kresge, A. J. *Can. J. Chem.* **1993**, *71*, 38–41. (e) Chiang, Y.; Eliason, R.; Guo, G. H.-X.; Kresge, A. J. *Can. J. Chem.* **1994**, *72*, 1632–1636.

(23) (a) Gold, V.; Waterman, D. C. A. *J. Chem. Soc. B* **1968**, 839–849. (b) Gold, V.; Waterman, D. C. A. *J. Chem. Soc. B* **1968**, 849–855. (24) Kresge, A. J. *Pure Appl. Chem.* **1964**, *8*, 243–258.

(25) Kresge, A. J.; Chiang, Y. *J. Chem. Soc. B* **1967**, 58–61.

(26) It is reasonable to assume that the fractionation factors for all hydroxyl groups of the glucosyl residue remain constant at 1.0 during the activation of the substrate (ref 27).

(27) (a) Schowen, R. L. In *Isotope Effects on Enzyme-Catalyzed Reactions*; Cleland, W. W., O'Leary, M. H., Northrop, D. B., Eds.; University Park Press: Baltimore, 1977; pp 64–99. (b) Schowen, K. B. J. In *Transition States of Biochemical Processes*; Gandour, R. D., Schowen, R. L., Eds.; Plenum: New York, 1978; pp 225–283.

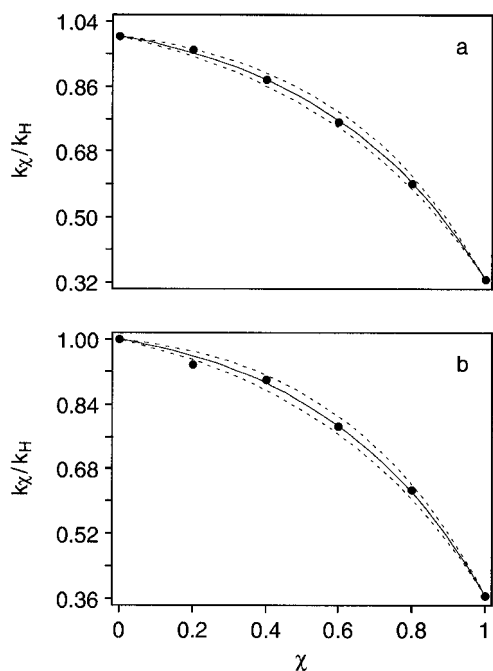


Figure 4. Relationship between the apparent solvent isotope effect, k_D/k_H , and the mole fraction deuterium content of the solvent, χ , for the hydrolysis of (a) **1** and (b) **2**. The solid lines represent the values of α determined by nonlinear regression while the dashed lines represent $\alpha \pm 0.1$.

mixtures of H_2O and D_2O containing 1 mM perchloric acid provided k_D/k_H . Nonlinear regression of eq 1 to the curved relationship between k_D/k_H and χ depicted in Figure 4 gave $\alpha = 0.627 \pm 0.013$ for **1** and $\alpha = 0.646 \pm 0.031$ for **2**. Thus, within experimental error, the values of α for **1** and **2** are the same.

$$\frac{k_D}{k_H} = \frac{(1 - \chi + \chi\lambda^{1-\alpha})^2(1 - \chi + \chi\lambda^{2\alpha+1}k_D/k_H)}{(1 - \chi + \chi\lambda)^3} \quad (1)$$

Spectroscopic Data. Because the mechanism of hydrolysis of **1** and **2** involves rate-limiting *C*-protonation, the difference in reactivity between **1** and **2** implies a difference in kinetic basicity between the two compounds. Although solvent deuterium isotope effects and α coefficients for general acid catalysis indicate little basis for the difference in kinetic basicity and reactivity, spectroscopic methods were expected to be considerably more sensitive probes of the ground-state electronic structures of the isopropenyl ether moieties of **1** and **2**. It was expected that the more reactive compound, **1**, would show evidence of greater conjugation in the isopropenyl ether and hence greater electron density on the β carbon of the double bond than **2**. The endocyclic $n_O \rightarrow \sigma^*_{CO}$ interaction that is present in **1** but absent in **2**^{13–15} should lengthen the glycosidic C–O bond and shorten the endocyclic C(1)–O(5) bond,²⁸ thereby raising the energy of the C(1)–O(5) σ^* orbital. The consequent reduction in the exocyclic $n \rightarrow \sigma^*$ interaction between the glycosidic oxygen and the

C(1)–O(5) bond would leave the glycosidic oxygen of **1** more available for conjugation with its attached isopropenyl group than is the glycosidic oxygen of **2**.

Indeed, UV spectra indicate greater conjugation in the isopropenyl ether of **1** than in the isopropenyl ether of **2**. Although both compounds exhibit absorbance maxima for the isopropenyl ether at 193 nm, the molar absorptivities of **1** and **2** are 4963 and 6473 $M^{-1} cm^{-1}$, respectively. By comparison, the molar absorptivities for 2-methyl-5,6-dihydropyran (**7**) and 9-oxabicyclo[3.3.1]non-1-ene (**8**) at $\lambda_{max} = 190$ nm are 5700 and 6200 $M^{-1} cm^{-1}$, respectively.²⁹ Because of conformational restrictions in **8**, the lone-pair electrons on oxygen are clearly less conjugated with the carbon–carbon double bond than are those in **7**. The less conjugated vinyl ether has the greater molar absorptivity.



¹H NMR shows a clear correlation between the reactivity and spectroscopic behavior of **1** and **2** and those of a series of simple alkyl vinyl ethers. While the difference in ¹H NMR chemical shift ($\Delta\delta_H$) between the terminal methylene protons of **1** is greater than that of **2**, the geminal coupling constant ($^2J_{HH}$) between the same protons is less negative in **1** than in **2** (Table 2). Similarly, the terminal vinyl protons of a series of simple alkyl vinyl ethers, $ROCH=CH_2$, in which R is *tert*-butyl, isopropyl, and methyl, display a trend toward decreasing difference in chemical shift but increasingly negative geminal coupling constant.³¹ The same series of vinyl ethers decreases in its reactivity toward acid-catalyzed hydrolysis (Table 2),³⁰ as well as cationic olefin polymerization.^{32,36}

Comparison of 2-chloroethyl vinyl ether with the other simple alkyl vinyl ethers in Table 2 suggests that *tert*-butyl vinyl ether is the most reactive of the simple alkyl vinyl ethers because its alkyl group is most electron releasing and allows the greatest resonance between oxygen and the carbon–carbon double bond. This interpretation is supported by kinetic and spectroscopic data for aryl vinyl ethers, which also show a correlation between decreasing rate of acid-catalyzed hydrolysis, decreasing difference in methylene proton chemical shifts, and increasingly negative geminal coupling constant between methylene protons (Table 2, Figure 5).

There are, however, some significant differences between the spectroscopic data for the simple alkyl vinyl ethers and those for the aryl vinyl ethers. The decreasing difference in chemical shift between the methylene protons of alkyl vinyl ethers is due, in general, to an

(29) Quinn, C. B.; Wiseman, J. R. *J. Am. Chem. Soc.* **1973**, *95*, 1342–1343.

(30) Ledwith, A.; Woods, H. J. *J. Chem. Soc. B* **1966**, 753–757.

(31) Feeney, J.; Ledwith, A.; H., S. L. *J. Chem. Soc.* **1962**, 2021–2023.

(32) Masuda, T. *J. Polym. Sci., Polym. Chem. Ed.* **1973**, *11*, 2713–2717.

(33) Potts, W. J.; Nyquist, R. A. *Spectrochim. Acta* **1959**, 679–708.

(34) McClelland, R. A. *Can. J. Chem.* **1977**, *55*, 548–551.

(35) Afonin, A. V.; Vashchenko, A. V.; Fujiwara, H. *Bull. Chem. Soc. Jpn.* **1996**, *69*, 933–945. We thank Professor Fujiwara for kindly providing us with the Supporting Information for this paper.

(36) Yuki, H.; Hatada, K.; Takeshita, M. *J. Polym. Sci., Part A-1* **1969**, *7*, 667–678.

(28) (a) Altona, C.; Romers, C. *Acta Crystallogr.* **1963**, *16*, 1225–1232. (b) Paulsen, H.; Luger, P.; Heiker, F. R. In *Anomeric Effect: Origin and Consequences*; Szarek, W. A., Horton, D., Eds.; ACS Symposium Series 87; American Chemical Society: Washington, DC, 1979; Chapter 5, pp 63–79. (c) Briggs, A. J.; Glenn, R.; Jones, P. G.; Kirby, A. J.; Ramaswamy, P. *J. Am. Chem. Soc.* **1984**, *106*, 6200–6206. (d) Jones, P. G.; Kirby, A. J. *J. Chem. Soc., Chem. Commun.* **1986**, 444–445.

Table 2. Correlation between Rates of Hydrolysis and Spectroscopic Data for the Methylidene Group of Vinyl Ethers

vinyl ether	k_{rel}	$\delta_{\text{H}_{\text{cis}}}$	$\delta_{\text{H}_{\text{trans}}}$	$\Delta\delta_{\text{H}}$	${}^2J_{\text{HH}}$, Hz	$\delta_{\text{C}_{\alpha}}$	$\delta_{\text{C}_{\beta}}$	${}^1J_{\text{CH}}$, Hz	$\nu_{\text{CH}}(\text{wag})$, cm^{-1}
1	100 ^a	4.35	4.22	0.13	-1.6	157.7	87.3	156.9, 160.7	825
2	29 ^a	4.29	4.23	0.06	-2.2	158.3	87.0	157.6, 161.2	812
<i>t</i> BuOCH=CH ₂	100 ^b	4.20 ^c	3.85 ^c	0.35	-0.1 ^c	146.7 ^d	91.2 ^d		824 ^e
<i>i</i> PrOCH=CH ₂	39 ^b	4.15 ^c	3.88 ^c	0.27	-1.2 ^c	150.9 ^d	88.1 ^d		810, 823 ^e
CH ₃ OCH=CH ₂	2.5 ^b	4.00 ^c	3.85 ^c	0.15	-2.2 ^c	153.0 ^d	86.1 ^d		813 ^e
ClCH ₂ CH ₂ OCH=CH ₂		4.05 ^c	4.17 ^c	0.12	-2.7 ^c				
<i>p</i> -CH ₃ O(C ₆ H ₄)OCH=CH ₂	100 ^f	4.60 ^g	4.28 ^g	0.32	-1.5 ^g	149.6 ^g	93.6 ^g	157.6, 161.6 ^g	
<i>p</i> -CH ₃ (C ₆ H ₄)OCH=CH ₂	76 ^f	4.67 ^g	4.33 ^g	0.34	-1.6 ^g	148.8 ^g	94.3 ^g	157.7, 161.6 ^g	
C ₆ H ₅ OCH=CH ₂	48 ^f	4.69 ^g	4.35 ^g	0.34	-1.5 ^g	148.4 ^g	95.1 ^g	157.9, 161.8 ^g	
<i>p</i> -Cl(C ₆ H ₄)OCH=CH ₂	15 ^f	4.72 ^g	4.41 ^g	0.31	-1.8 ^g	148.0 ^g	95.8 ^g	158.3, 162.1 ^g	
<i>p</i> -O ₂ N(C ₆ H ₄)OCH=CH ₂	1.1 ^f	4.97 ^g	4.68 ^g	0.29	-2.0 ^g	146.1 ^g	99.1 ^g	159.3, 162.8 ^g	

^a Relative k_{H^+} for hydrolysis in water at 25 °C. ^b Relative k_{H^+} for hydrolysis in 95% aqueous acetone at 25 °C (ref 30). ^c Reference 31. ^d Calculated from chemical shifts reported in ref 32, assuming that $\delta_{\text{C}}(\text{CS}_2) = 193.7$. ^e Reference 33. ^f Relative rate of hydrolysis in 1.00 N HCl at 25 °C (ref 34). ^g Reference 35.

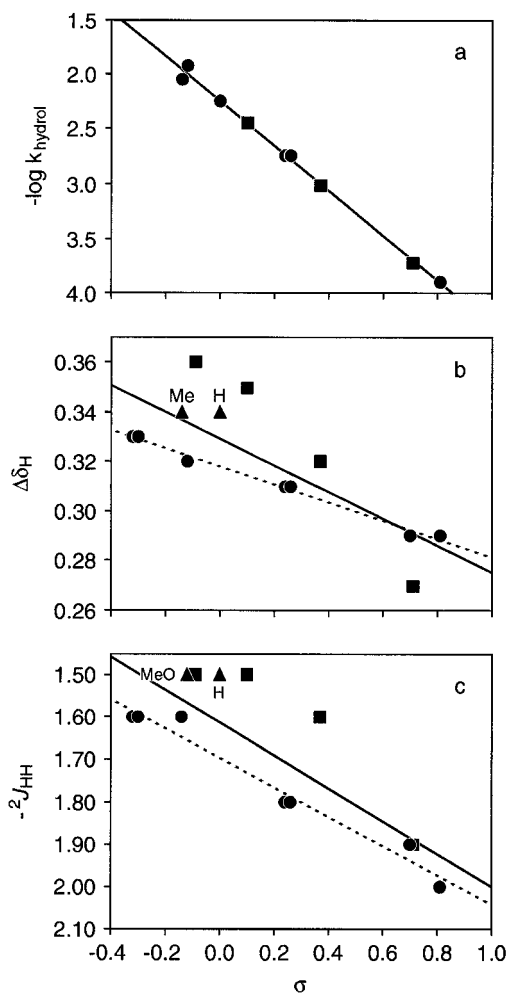


Figure 5. Hammett correlations for (a) the rates of acid-catalyzed hydrolysis, (b) the differences in ¹H NMR chemical shift ($\Delta\delta_{\text{H}} = \delta_{\text{H}_{\text{cis}}} - \delta_{\text{H}_{\text{trans}}}$) between terminal methylidene protons, and (c) the geminal coupling constants (${}^2J_{\text{HH}}$) between terminal methylidene protons of substituted aryl vinyl ethers. Aryl substituents are *para* (circles) or *meta* (squares). Triangles represent *para*-substituted or unsubstituted aryl vinyl ethers that generated anomalous data. Solid lines are the best least-squares fits to all data. Dashed lines are the best least-squares fits to only the data represented by circles. Data taken from ref 35.

upfield shift of the signal for the proton *cis* to the alkoxy group ($\delta_{\text{H}_{\text{cis}}}$). With the aryl vinyl ethers, however, NMR signals for both methylidene protons shift downfield as

the aryl group becomes more electron deficient and the vinyl ether becomes less reactive. The general decrease in chemical shift difference between methylidene protons results from a greater downfield shift of the signal for the proton *trans* to the aryloxy group ($\delta_{\text{H}_{\text{trans}}}$). Although Hammett σ values and the rates of hydrolysis of both *para*- and *meta*-substituted aryl vinyl ethers correlate well, Hammett plots of the ¹H NMR data for the same aryl vinyl ethers show considerable scatter (Figure 5). *Meta* substituents, in particular, influence $\Delta\delta_{\text{H}}$ and ${}^2J_{\text{HH}}$ more strongly than *para* substituents. In addition, phenyl and *p*-methylphenyl vinyl ethers in the case of $\Delta\delta_{\text{H}}$ or phenyl and *p*-methoxyphenyl vinyl ethers in the case of ${}^2J_{\text{HH}}$ lie significantly off the line defined by other *para*-substituted phenyl vinyl ethers. It should be noted that the trends in $\Delta\delta_{\text{H}}$ and ${}^2J_{\text{HH}}$ exhibited by aryl vinyl ethers are opposite from those predicted by the assumption that increased electron donation from the ethereal oxygen leads to greater $\text{sp}^2 \rightarrow \text{sp}^3$ rehybridization of the methylidene carbon.³⁰ Such rehybridization would lead to decreased $\Delta\delta_{\text{H}}$ (as the protons become more magnetically equivalent) and to more negative ${}^2J_{\text{HH}}$.³⁷

Although ¹³C NMR has been used previously to examine vinyl ethers^{32,35,38} and is considered to be a sensitive probe of hybridization and electron density associated with individual carbon atoms,³⁹ **1** and **2** exhibit only small differences between the chemical shifts ($\delta_{\text{C}_{\alpha}}$ and $\delta_{\text{C}_{\beta}}$) and one-bond ¹³C-¹H coupling constants (${}^1J_{\text{CH}}$) of their isopropenyl ether moieties (Table 2). Still, the differences in ¹³C NMR chemical shift between **1** and **2** correlate with those of the alkyl vinyl ethers in Table 2. As the vinyl ether becomes more reactive, $\delta_{\text{C}_{\alpha}}$ shifts upfield and $\delta_{\text{C}_{\beta}}$ shifts downfield. For aryl vinyl ethers, however, the trend is exactly opposite, with $\delta_{\text{C}_{\alpha}}$ shifting downfield and $\delta_{\text{C}_{\beta}}$ shifting upfield as the reactivity of the vinyl ether increases (Table 2, Figure 6). Nevertheless, the trend in one-bond ¹³C-¹H coupling constants for the methylidene groups of **1** and **2** agrees with that of the aryl vinyl ethers. As the reactivity of the vinyl ether increases, both values of ${}^1J_{\text{CH}}$ decrease (Table 2, Figure 6). Although the correlations between reactivity and ¹³C

(37) Pople, J. A.; Bothner-By, A. A. *J. Chem. Phys.* **1965**, *42*, 1339-1349.

(38) Reynolds, W. F.; McClelland, R. A. *Can. J. Chem.* **1977**, *55*, 536-540.

(39) (a) Hansen, P. E. *Prog. Nucl. Magn. Reson. Spectrosc.* **1981**, *14*, 175-296. (b) Webb, J. G. K.; Yung, D. K. *Can. J. Chem.* **1983**, *61*, 488-493. (c) Tolman, C. A.; English, A. D.; Manzer, L. E. *Inorg. Chem.* **1975**, *14*, 2353-2356.

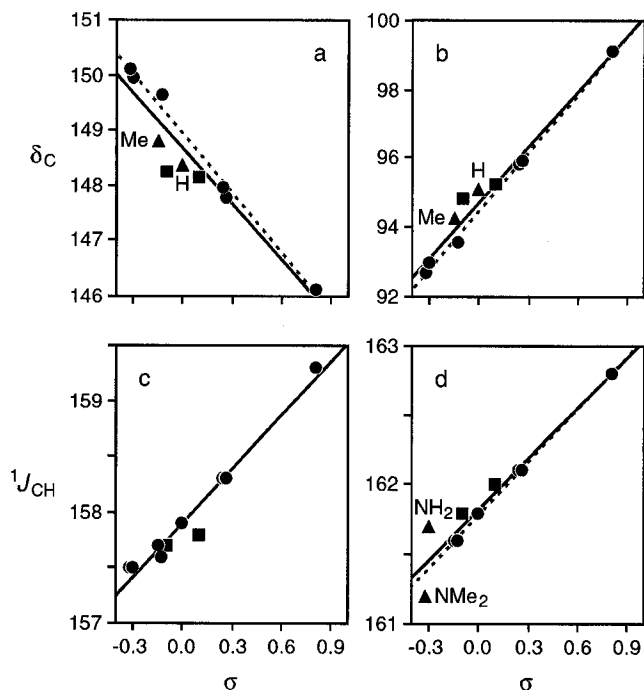


Figure 6. Hammett correlations for (a) the ^{13}C NMR chemical shifts of the α vinyl carbon atoms, (b) the ^{13}C NMR chemical shifts of the β vinyl carbon atoms, (c) the one-bond ^{13}C – ^1H coupling constants between the β vinyl carbon atoms and the protons cis to the aryloxy groups ($^1J_{\text{CH}^{\text{cis}}}$), and (d) the one-bond ^{13}C – ^1H coupling constants between the β vinyl carbon atoms and the protons trans to the aryloxy groups ($^1J_{\text{CH}^{\text{trans}}}$) of substituted aryl vinyl ethers. See Figure 5 for an explanation of the symbols used. Data taken from ref 35.

NMR data are better than those involving ^1H NMR data, for ^{13}C NMR chemical shifts, it is again phenyl and *p*-methylphenyl vinyl ethers that deviate from the trends established by the other aryl vinyl ethers. In the Hammett plot of $^1J_{\text{CH}^{\text{trans}}}$, *p*-amino- and *p*-(dimethylamino)phenyl vinyl ethers are the notable outliers.

In the IR, the methylene protons of **1** and **2** exhibit the same trend in their strong, out-of-plane wagging frequencies as do the methylene protons of the simple alkyl vinyl ethers in Table 2. The more reactive vinyl ethers display higher methylene wagging frequencies. In the case of the simple alkyl vinyl ethers, the different wagging frequencies have been interpreted as representing different conformers about the alkyl³³ or vinyl⁴⁰ C–O bond. Methyl vinyl ether is believed to exist in the *s-cis* conformation while *tert*-butyl vinyl ether is believed to exist in a *gauche* conformation. Isopropyl vinyl ether displays two methylene wagging frequencies because it exists as an approximately 1:1 mixture of two possible conformers.

Conclusion

All experimental evidence indicates that the hydrolyses of **1** and **2** proceed by irreversible, rate-limiting C-protonation, followed by alkenyl ether C–O bond cleavage, not glycosidic C–O bond cleavage. Compounds **1** and **2** are the first vinyl acetals demonstrated to hydrolyze exclusively by cleavage of the vinyl ether C–O bond. The magnitudes of both the solvent deuterium kinetic isotope effects and the α coefficients for general acid

catalysis indicate a relatively late transition state with significant transfer of an acidic proton to the β -carbon of the vinyl ether.

Because protonation of the alkenyl ether is involved in the rate-limiting step of hydrolysis, the greater reactivity of **1** indicates that **1** is kinetically more basic than **2**. This assertion is supported by the fact that the enthalpy of activation for the hydrolysis of **1** is significantly lower than that for the hydrolysis of **2**. The lower activation barrier of **1** is partially offset by a more negative entropy of activation. Presumably, the more sterically encumbered isopropenyl group of **1** requires greater increase in order upon protonation and nucleophilic attack than does that of **2**.

The cause for the greater kinetic basicity of **1** cannot be steric accessibility of the enol ether or dipole–dipole interactions within the substrate since both of these should make **2** more reactive than **1**. The difference in UV molar absorptivities of **1** and **2** clearly indicates a difference in the extent of conjugation of the glycosidic oxygens with their attached alkenyl double bonds. However, comparison of **1** and **2** with **7** and **8** suggests that the difference in conjugation is due to a conformational difference, not a difference in the electronic states of the glycosidic oxygens. ^1H NMR and ^{13}C NMR spectroscopies show parallels between the reactivities and spectroscopic properties of isopropenyl glucopyranosides and those of simple alkyl vinyl ethers and substituted aryl vinyl ethers. These similarities indicate that electron donation from the glycosidic oxygen into the alkenyl ether double bond by resonance is greater in **1** than in **2**. Trends in ^{13}C NMR chemical shift data, however, suggest that the difference in reactivity between **1** and **2** originates from steric constraints. Correlations between the reactivity and ^{13}C NMR chemical shifts of **1** and **2** are identical with those of simple alkyl vinyl ethers but opposite of those of substituted aryl vinyl ethers (Table 2). While the difference between aryl vinyl ethers is certainly electronic, the major difference between the simple alkyl vinyl ethers is the size of the alkyl group and any change in ground-state conformational population that might attend changes in steric strain. Even the differences in ^1H NMR chemical shift between methylene protons show greater similarity between the isopropenyl glucosides and alkyl vinyl ethers than between the isopropenyl glucosides and aryl vinyl ethers. Similarities in the IR between the methylene wagging frequencies of **1** and **2** and those of *tert*-butyl and methyl vinyl ethers also indicate that the increased reactivity of **1** is due to an effect of sterics on the ground-state conformation or stability. Thus, while various spectroscopic evidence indicates a difference in the degree of conjugation within the enol ether moieties of **1** and **2**, it appears that the increased reactivity of **1** is due more to steric and conformational strain in the ground state than to a difference in the electronic states of the glycosidic oxygen atoms of **1** and **2** resulting from $n_{\text{O}} \rightarrow \sigma^*_{\text{CO}}$ interactions.

Experimental Section

General Procedures. Anhydrous methanol was used as purchased from Aldrich. Enzymes from Sigma and Biozyme and other reagents were used as purchased. Synthetic reactions were performed under an inert atmosphere of dry argon, using dry glassware and standard syringe/septa techniques. Analytical TLC was performed on plates (Whatman or Analtech) containing a 250 μm -thick layer of 60 Å silica gel.

(40) Ledwith, A.; Woods, H. J. *J. Chem. Soc. B* **1970**, 310–314.

Compounds were visualized by dipping plates into *p*-anisaldehyde stain and heating. Preparative liquid chromatography was performed on 230–400 mesh 60 Å silica gel (Aldrich).

¹H NMR spectra were obtained at a nominal resonance frequency of 250 MHz, using D₂O as solvent and sodium 3-(trimethylsilyl)propionate-2,2,3,3-*d*₄ (TSP) as the internal reference (δ 0.00 ppm). Liquid secondary ion mass spectroscopy (LSIMS) was performed using Cs⁺ (20 eV) as the ionizing beam and glycerol/NaI as the matrix. Elemental analysis was performed by Robertson Microlit Laboratories, Inc.

Kinetic experiments were maintained at constant temperature by a digital Peltier controller. Disappearance of the vinyl ether functional group was observed spectroscopically by the decrease in absorbance at λ = 215 nm. Apparent rate constants were calculated by nonlinear regression of UV/vis data, using Enzfitter version 1.05 software.

Isopropenyl α-D-Glucopyranoside (1). To 1.00 g (1.80 mmol) of isopropenyl 2,3,4,6-tetra-*O*-pivaloyl-α-D-glucopyranoside³ in 5 mL of methanol was added 0.360 mL of a 20% solution of sodium methoxide in methanol. The reaction was stirred overnight at room temperature. Dowex-50W×8 resin (H⁺, 0.300 g) was added to the solution, and the solution was filtered quickly. The solvent was evaporated in vacuo to afford a white solid. Purification by flash chromatography using chloroform/ethyl acetate/methanol (5:2:1) as the eluent yielded 0.325 g (82%) of **1**: mp 157–159 °C; *R*_f 0.84 (80% aqueous acetonitrile containing 9.5 mM tetrabutylammonium hydroxide); ¹H NMR δ 5.45 (d, *J* = 3.7 Hz, 1H), 4.35 (d, *J* = 1.7 Hz, 1H), 4.22 (dq, *J* = 0.8, 1.7 Hz, 1H), 3.85–3.61 (m, 5H), 3.46 (t, *J* = 9.4 Hz, 1H), 1.88 (s, 3H); ¹³C NMR δ 157.7, 95.2, 87.3, 73.4, 72.6, 71.3, 69.7, 60.7, 19.7; IR (KBr) 3456 (s), 3247 (s), 2926 (m), 1654 (w), 1637 (m), 1274 (s), 1145 (m), 1112 (s), 1086 (m), 1053 (s), 1034 (s), 825 (s) cm⁻¹; LSIMS *m/z* 243 (M + Na⁺), 163, 145, 127, 109. Anal. Calcd for C₉H₁₆O₆: C, 49.09; H, 7.32. Found: C, 49.15; H, 7.54.

Isopropenyl β-D-Glucopyranoside (2). To 1.00 g (2.59 mmol) of isopropenyl 2,3,4,6-tetra-*O*-acetyl-β-D-glucopyranoside³ in 10 mL of methanol was added 0.300 mL of a 20% solution of sodium methoxide in methanol. After 8 h, the reaction was quenched with 0.100 g of Dowex-50W×8 resin, and the solution was filtered quickly. The solvent was evaporated in vacuo. Purification of the white solid by flash chromatography using chloroform/ethyl acetate/methanol (5:2:1) as the eluent yielded 0.541 g (95%) of **2**: mp 137–138 °C; *R*_f 0.78 (80% aqueous acetonitrile containing 9.5 mM tetrabutylammonium hydroxide); ¹H NMR (D₂O) δ 4.94 (d, *J* = 7.8 Hz, 1H), 4.29 (d, *J* = 2.2 Hz, 1H), 4.23 (dq, *J* = 0.8, 2.2 Hz, 1H), 3.92 (dd, *J* = 2.1, 12.4 Hz, 1H), 3.72 (dd, *J* = 5.6, 12.4 Hz, 1H), 3.61–3.54 (m, 2H), 3.47–3.39 (m, 2H), 1.88 (d, *J* = 0.54 Hz, 3H); ¹³C NMR δ 158.3, 98.5, 87.0, 76.4, 75.9, 73.0, 69.8, 61.0, 19.7; IR (KBr) 3446 (s), 2927 (m), 1654 (m), 1637 (m), 1560 (w), 1508 (w), 1374 (m), 1271 (s), 1106 (s), 1073 (s), 1019 (s), 812 (s) cm⁻¹; LSIMS *m/z* 243 (M + Na⁺), 163, 145, 127, 109. Anal. Calcd for C₉H₁₆O₆: C, 49.09; H, 7.32. Found: C, 48.92; H, 7.50.

Hydrolysis of 1 and 2 Monitored by ¹H NMR. A 10 mM sodium salicylate buffer, pH 3.0, in D₂O was prepared by dissolving 69.0 mg (0.500 mmol) of salicylic acid in 40 mL of D₂O, adjusting the pH to 3.0 with 1 M NaOD in D₂O, and adding D₂O to bring the final volume to 50 mL. In an NMR tube, 600 μL of salicylate buffer was added to 50 μL of 364 mM isopropenyl glucopyranoside in D₂O. Hydrolysis of the glucopyranoside was monitored by acquisition of ¹H NMR spectra and observing the disappearance of the anomeric proton of **1** or **2** and the appearance of the anomeric proton of α- or β-glucopyranose, respectively.

Methanolysis of 1 and 2. A 25 mM solution of DCl in methanol-*d*₄ was prepared by adding 3.0 μL of benzoyl chloride to 977 μL of methanol-*d*₄. In an NMR tube, 4.0 mg of isopropenyl glucopyranoside was dissolved in 625 μL of methanol-*d*₄, and an ¹H NMR spectrum was obtained. After the addition of 25 μL of 25 mM DCl in methanol-*d*₄ to the glucopyranoside solution, subsequent ¹H NMR spectra were acquired.

Hydrolysis of 1 and 2 in H₂¹⁸O. Isopropenyl glucopyranoside (1.0 mg) was dissolved in 100 μL of 10 mM chloroacetate buffer, pH 3.0, prepared in 97.9% H₂¹⁸O. Hydrolysis of each glucopyranoside was monitored by GC–MS and electrospray-MS. Aliquots (10 μL) of each reaction were removed periodically, added to a microcentrifuge tube, and extracted with CHCl₃ (10 μL). Portions of the CHCl₃ solutions were removed by syringe and used to monitor the formation of acetone by GC–MS. Aliquots (10 μL) of the reactions were also removed to monitor the formation of glucose by electrospray-MS.

Solvent Deuterium Incorporation during Hydrolysis of 1 and 2. Isopropenyl glucopyranoside (4.0 mg) was dissolved in 650 μL of 10 mM chloroacetate buffer in D₂O, pH 3.0, and hydrolysis was monitored by ¹H NMR. Aliquots (10 μL) of each reaction were removed periodically and extracted with CHCl₃ (10 μL). Portions of the CHCl₃ solutions were analyzed by GC–MS to monitor the formation of acetone.

Hydronium Ion Catalytic Coefficients and Solvent Isotope Effects. Rates of hydrolysis of **1** and **2** were measured at 25 °C in solutions of 0.50, 1.00, 2.00, or 4.00 mM perchloric acid made in H₂O or D₂O. Values of *k*_{H⁺} and *k*_{D⁺} were calculated by linear regression of the averages of triplicate determinations of the apparent rate constant at each concentration of perchloric acid.

Apparent solvent isotope effects in isotopically mixed solvents were determined by mixing the appropriate amounts of 1.00 mM perchloric acid in H₂O and 1.00 mM perchloric acid in D₂O and measuring the rates of hydrolysis of **1** and **2** at 25 °C. Rates of hydrolysis at each ratio of H₂O and D₂O were determined in quadruplicate and averaged.

Buffer Dilution Studies. Rates of hydrolysis of **1** and **2** were determined in a series of carboxylic acid buffer solutions of constant buffer ratio but varying buffer concentration. Chloroacetic acid, 3-chlorolactic acid, formic acid, glycolic acid, and propionic acid were used to make buffers. Buffers were constructed by mixing known quantities of each free acid with a standardized solution of sodium hydroxide. The “nominal pH” of each buffer was calculated from the proportions of free acid and sodium hydroxide mixed, using the Henderson–Hasselbalch equation. Each stock solution of buffer was diluted to various concentrations so as to maintain a constant nominal ratio of [HA]/[A⁻]. At low concentrations of buffer, however, this ratio declined due to dissociation of the free acid into A⁻ + H⁺ (buffer failure).⁴¹ All buffers were maintained at a constant ionic strength of 0.100 M by including sodium chloride in the stock solutions and dilutions, taking buffer failure into account in determining the degree of ionization of each carboxylic acid. Chloroacetate buffer was made fresh daily since it hydrolyzes upon sitting. All other buffers were used within 3–4 days of being made.

The observed rate constants for hydrolysis of **1** and **2** were adjusted for the decrease in hydronium ion concentration at low concentrations of buffer due to buffer failure, using the method of Kresge (eq 2).⁴¹ The observed rate constants, *k*_{obs},

$$k_{\text{adj}} = k_{\text{obs}} + ([\text{H}^+]_{\text{max}} - [\text{H}^+]_{\text{act}})k_{\text{H}^+} \quad (2)$$

$$[\text{H}^+]_{\text{act}} = \frac{-(\gamma_{\text{H}} + \gamma_{\text{A}^-})[\text{A}^-]_{\text{nom}} + K_{\text{a}} + \sqrt{((\gamma_{\text{H}} + \gamma_{\text{A}^-})[\text{A}^-]_{\text{nom}} + K_{\text{a}})^2 + 4\gamma_{\text{H}^+}\gamma_{\text{A}^-} - [\text{HA}]_{\text{nom}}K_{\text{a}}}}{2\gamma_{\text{H}^+}\gamma_{\text{A}^-}} \quad (3)$$

$$[\text{HA}]_{\text{act}} = [\text{HA}]_{\text{nom}} - [\text{H}^+]_{\text{act}} \quad (4)$$

$$k_{\text{adj}} = k_{\text{H}^+}[\text{H}^+]_{\text{act}} + k_{\text{HA}}[\text{HA}]_{\text{act}} \quad (5)$$

measured at various concentrations of a given buffer were adjusted to the hydronium ion concentration of the most concentrated buffer ([H⁺]_{max}), using hydronium ion concentra-

(41) Kresge, A. J.; Chen, H. L.; Chiang, Y.; Murrill, E.; Payne, M. A.; Sagatys, D. S. *J. Am. Chem. Soc.* **1971**, *93*, 413–423.

tions ($[H^+]_{act}$) calculated from acid dissociation constants (eq 3) and the hydronium ion catalytic coefficients (k_{H^+}) reported in Table 1. Activity coefficients (γ_{H^+} and γ_{A^-}) of 0.83 and 0.78 were used for hydronium and carboxylate ions, respectively, at an ionic strength 0.100 M.⁴² The actual concentrations of carboxylic acid present in solution were calculated by adjusting for depletion due to dissociation (eq 4). The adjusted rate constants and actual concentrations of general acid were then fit to eq 5 by linear regression.

Acknowledgment. We thank Dr. Gordon Nicol for providing LSIMS data and for help with the GC-MS

and electrospray-MS experiments. We thank Jie Yang for acquiring the proton-coupled ¹³C NMR spectra of **1** and **2**.

Supporting Information Available: Partial assignments of ¹H and ¹³C NMR spectra of **1** and **2**, as well as tables of rate data versus temperature, concentration of hydronium ion, solvent deuterium content, and concentration of buffer (3 pages). This material is contained in libraries on microfiche, immediately follows this article in the microfilm version of the journal, and can be ordered from the ACS; see any current masthead page for ordering information.

(42) Kielland, J. *J. Am. Chem. Soc.* **1937**, *59*, 1675–1678.